

# A Closely-Coupled Pyrene Dimer Having Unusually Intense Fluorescence

Andrew C. Benniston,<sup>\*[a]</sup> Anthony Harriman,<sup>[a]</sup> Donald J. Lawrie,<sup>[a]</sup> and Sarah A. Rostron<sup>[a]</sup>

**Keywords:** Fluorescence / Sensors / Pyrene / Charge transfer / Glaser coupling

A synthetic route is described for the preparation of 1,4-di(1-pyrenyl)butadiyne. The target compound, after purification by extensive column chromatography, has been characterized by NMR and exact-mass spectrometry. This material is highly-fluorescent in solution and, relative to pyrene, strongly absorbing in the near-UV region. Phosphorescence is observed at 77 K and formation of the metastable triplet

state has been confirmed by laser flash photolysis. In marked contrast to pyrene, fluorescence from the target compound is not susceptible to self-quenching nor to the presence of dissolved oxygen. The average conformation of the molecule has been established by molecular modeling.  
(© Wiley-VCH Verlag GmbH & Co. KGaA, 69451 Weinheim, Germany, 2004)

## Introduction

Pyrene is the archetypal fluorescent polycycle. It has been examined in a bewildering variety of environments<sup>[1]</sup> and innumerable analytical protocols have been developed based on induced changes in its fluorescence yield.<sup>[2–7]</sup> Despite its enormous popularity, there are several serious drawbacks with the photophysical properties of pyrene that restrict its application in molecular photonic devices. The most important limitations relate to the poor absorption profile,<sup>[8]</sup> the susceptibility towards excimer formation,<sup>[9]</sup> oxygen quenching of the fluorescence intensity<sup>[10]</sup> and the relatively low fluorescence quantum yield.<sup>[11]</sup> Of course, pyrene exhibits many beneficial properties such as its ready functionalization<sup>[12]</sup> and appearance of delayed fluorescence<sup>[13]</sup> that add to its attractiveness as a fluorescent tag. We now describe a simple derivative of pyrene that displays improved optical properties in solution. The target compound is formed by attaching pyrenyl residues to each end of a butadiynylene spacer. The result is a highly fluorescent compound which could form the basis of more complex assemblies.

In carrying out this work we have also sought to address a further issue of contemporary importance. This concerns seeking an improved understanding of the photophysics of closely-coupled chromophores.<sup>[14]</sup> The main issue here relates to distinguishing between adjacent but discrete chromophores and large molecules. The latter species share LUMOs and HOMOs across the molecule and the molecular properties are quite disparate from those of the individ-

ual chromophores. Because of the rapid growth in the use of conjugated molecules for miniaturized optical devices,<sup>[15]</sup> it is important to assess the boundaries of the chromophore. The target compound synthesized herein is a prime candidate for such studies. Indeed, it is concluded that the two pyrenyl groups act cooperatively and combine to form a single molecular entity.

## Results and Discussion

### Synthesis and General Properties

The synthesis of **1** (Figure 1) was carried out using the Glaser coupling of 1-ethynylpyrene, using a minor modification of the previously reported procedure.<sup>[16]</sup> The purification of **1** required at least two chromatographic separations (silica gel, petrol: ethyl acetate), followed by preparative TLC, in order to obtain a spectroscopically pure material. It was noted that the <sup>1</sup>H NMR spectrum of the product at each stage of purification did not show any dramatic changes; the critical protocol adapted by us to measure improvements in purity involved comparing excitation and fluorescence spectra. In particular, the fluorescence excitation spectrum became better resolved at each stage of purification. The aromatic proton signals for the pyrene residues are well-resolved in the <sup>1</sup>H NMR spectra. Moreover, the spectra recorded at different concentrations in CDCl<sub>3</sub> (about 3–30 mM) did not undergo any significant chemical shifts. This observation suggests that **1** undergoes negligible intermolecular  $\pi$ - $\pi$  stacking for the formation of a dimer in this concentration range. Compound **1** is soluble in a wide range of solvents of varying polarity, including protic and aprotic solvents. No observable changes occurred to solutions of **1** after exposure to ambient light for several weeks. Indeed, prolonged UV illumination of **1** in aerated ethanol solution had little effect on the absorption

<sup>[a]</sup> Molecular Photonics Laboratory, School of Natural Sciences (Chemistry), Bedson Building, University of Newcastle, Newcastle upon Tyne, NE1 7RU, United Kingdom  
Fax: (internat.) +44-191-222-8660  
E-mail: a.c.benniston@ncl.ac.uk

spectrum. It was noted that compound **1** coated the glassware with an intensely fluorescent film.

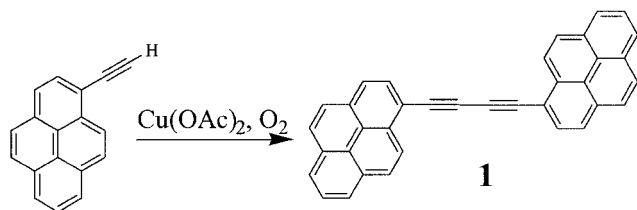


Figure 1. Preparation of **1** from 1-ethynylpyrene

The target compound **1** undergoes an irreversible one-electron oxidation step under cyclic voltammetric conditions. The peak potential lies at +1.70 V vs. Ag/AgCl in acetonitrile solution. There is no indication of a second oxidative process at potentials less than 2.0 V vs. Ag/AgCl. The peak potential is essentially unaffected by changes in solvent polarity, and is much more positive than that found for either pyrene ( $E_p = +1.10$  V vs. Ag/AgCl)<sup>[17]</sup> 1-ethynylpyrene ( $E_p = +1.47$  V vs. Ag/AgCl).<sup>[18]</sup> The irreversible nature of the electrode process arises because of the poor solubility of the resultant  $\pi$ -radical cation and its association with a ground-state molecule to form a dimer radical cation. A similar behavior has been reported for pyrene-ethynylene compounds used for chemical sensing applications.<sup>[19]</sup> In deoxygenated DMF solution, compound **1** undergoes two irreversible one-electron reductions with half-wave potentials ( $E_{1/2}$ ) of  $-1.45$  V vs. Ag/AgCl and  $-1.65$  V vs. Ag/AgCl, respectively. The first value can be compared with that observed for 1-ethynylpyrene, whose cyclic voltammogram shows a *quasi*-reversible one-electron reduction step with  $E_{1/2} = -1.78$  V vs. Ag/AgCl. Pyrene itself is reduced with  $E_{1/2} = -2.07$  V vs. Ag/AgCl. Thus, the net effect of the butadiynylene linker is to make the aromatic nucleus more difficult to oxidize but much easier to reduce. Both oxidation and reduction steps are restricted to one-electron processes occurring within a single molecular entity.

Molecular orbital calculations indicate that both the HOMO and LUMO of **1** cover the entire molecule (Figure 2). This suggests that **1** functions as a single molecular entity, rather than an accretion of individual subunits. Such behavior would explain why the oxidation and reduction steps are restricted to the removal and addition of a single electron, respectively. These calculations were also used to obtain the energy-minimized conformation of **1** in vacuo. It was found that the *cis*-conformation was slightly less stable than the corresponding *trans*-conformer (Figure 2), as formed by rotation around the central butadiynylene connector. The barrier for free rotation was computed to be  $7.5 \text{ kJ mol}^{-1}$ .

The absorption spectrum of pyrene in cyclohexane is well-resolved with the lowest-energy ( $^1L_b$ ) transition at  $28,169 \text{ cm}^{-1}$  (see a in Figure 3). This transition is very weak ( $\epsilon = 550 \text{ M}^{-1} \text{ cm}^{-1}$ ), but there are more intense transitions at around  $29,851 \text{ cm}^{-1}$  ( $^1L_a$ ) and  $36,765 \text{ cm}^{-1}$  ( $^1B_u$ ). In

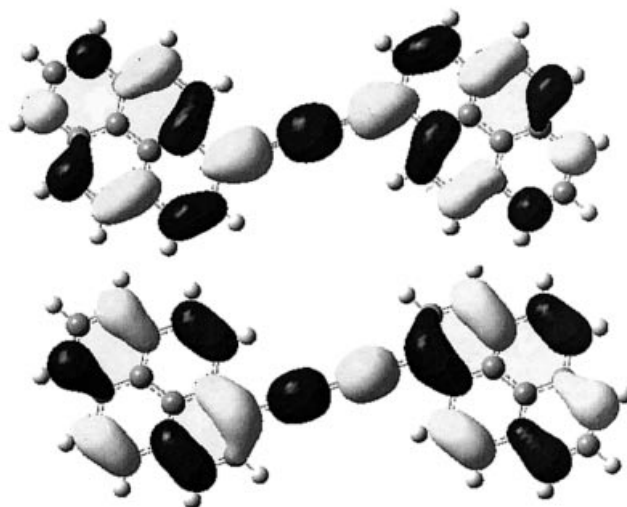


Figure 2. Pictorial representation of the calculated LUMO (top) and HOMO (bottom) orbitals of **1** in vacuo

marked contrast, **1** shows a broad and relatively intense ( $\epsilon = 8,315 \text{ M}^{-1} \text{ cm}^{-1}$ ) transition centered at  $25,000 \text{ cm}^{-1}$ . There are additional transitions across the range  $26,316$  to  $33,333 \text{ cm}^{-1}$  (see b in Figure 3) that are poorly resolved. The modest red-shift noted for the 0,0 absorption transition, taken together with the increased molar absorption coefficient, provides for a vastly improved absorption spectral profile and leads to a significant increase in the radiative rate constant. Thus, this latter parameter is raised from  $1.4 \times 10^6 \text{ s}^{-1}$  for pyrene to  $7.9 \times 10^8 \text{ s}^{-1}$  for **1** in cyclohexane solution. The oscillator strength calculated, assuming a single transition for the lowest-energy absorption of **1**, in cyclohexane is 0.143.

Fluorescence is readily observed from both pyrene and **1** in cyclohexane at ambient temperature (Figure 3). Emission from **1** is relatively broad and red-shifted. The 0,0 transitions are at  $25,316$  and  $22,727 \text{ cm}^{-1}$  for pyrene and **1**, respectively. For **1**, there is a small Stokes shift (approximately 37 nm) that remains essentially insensitive to changes in solvent polarity. This latter finding suggests that excitation does not cause a significant change in dipole moment. The fluorescence quantum yield ( $\Phi_F = 0.95 \pm 0.03$ ) recorded for **1** in deoxygenated cyclohexane is close to unity and is much higher than that found for pyrene ( $\Phi_F = 0.58$ ) under identical conditions. In fact,  $\Phi_F$  is found to be almost independent of solvent polarity and relatively unaffected by the presence of molecular oxygen. This latter observation is a consequence of the relatively short excited state lifetime ( $\tau_S = 1.2 \pm 0.1 \text{ ns}$ ) found for **1**. The short lifetime precludes intermolecular excimer formation in solution, such that the photophysical properties of **1** are found to be insensitive to changes in concentration. This is in marked contrast to the behavior of pyrene ( $\tau_S = 450 \text{ ns}$ ) which readily forms excimers in nonpolar solvents. The rigid connector bridge of **1** also precludes formation of an intramolecular excimer, a feature which occurs in dipyrrene compounds containing

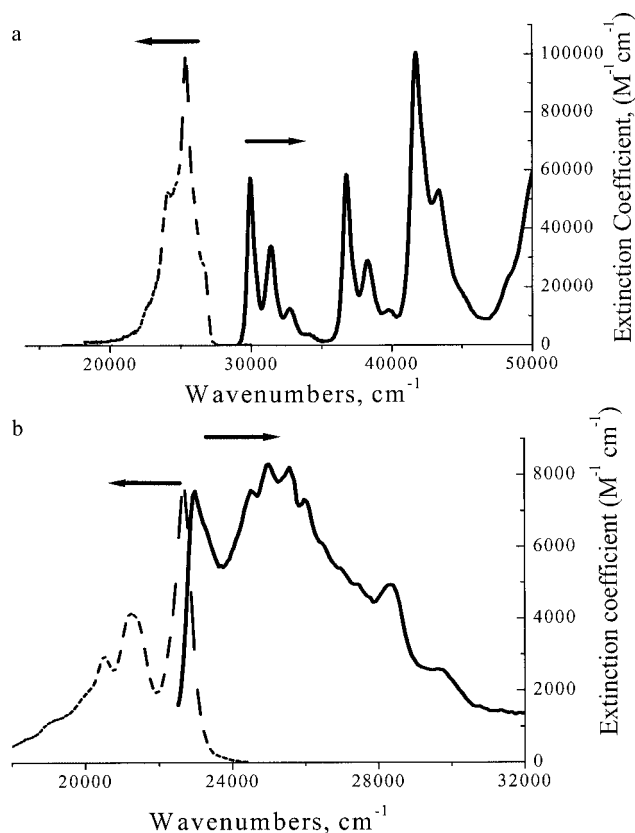


Figure 3. Absorption (dark line) and fluorescence (dashed line) profiles of (a) pyrene and (b) **1** in dilute cyclohexane at ambient temperature

flexibly saturated bridges.<sup>[20]</sup> Thus, it was found that the fluorescence decay curves recorded for **1** followed single-exponential kinetics in all solvents studied. The calculated radiative rate constant ( $k_f$ ) and non-radiative rate constant ( $k_{nr}$ ) for **1**,  $7.9 \times 10^8 \text{ s}^{-1}$  and  $43 \times 10^6 \text{ s}^{-1}$ , respectively, [Equation (1)] are notably larger than those found for pyrene ( $k_f = 1.3 \times 10^6 \text{ s}^{-1}$ ,  $k_{nr} = 92 \times 10^4 \text{ s}^{-1}$ ).

$$k_f = 1/\tau_s \text{ and } k_{nr} = 1/\tau_s - k_f \quad (1)$$

The increase in  $k_{nr}$  for **1** relative to pyrene is consistent with the lowering in energy of the singlet state, and can be explained in terms of the energy-gap law since coupling to the ground state is enhanced.<sup>[21]</sup>

Both pyrene and **1** phosphoresce at 77 K in the presence of iodoethane as a heavy-atom perturber. The 0,0 transition of the phosphorescence spectrum noted for **1** lies at  $15,038 \text{ cm}^{-1}$ , compared with a value of  $16,807 \text{ cm}^{-1}$  for pyrene. The phosphorescence yield found for **1** was, as expected, very low. Even so, the singlet-triplet energy gap could be calculated to be ca.  $7700 \text{ cm}^{-1}$ . Laser flash photolysis studies confirmed the formation of the triplet excited state in poor yield (Figure 4). The transient absorption profile is dominated by bleaching of the 300–450 nm region and a broad Gaussian band centered at ca. 680 nm. In compari-

son, the triplet-triplet absorption signal of pyrene in acetonitrile is at 412 nm.<sup>[22]</sup> In deoxygenated acetonitrile, the triplet lifetime was found to be  $25 \pm 4 \mu\text{s}$ . The transient absorption signal decayed cleanly via first-order kinetics and there was no indication for triplet-triplet annihilation at modest concentration.

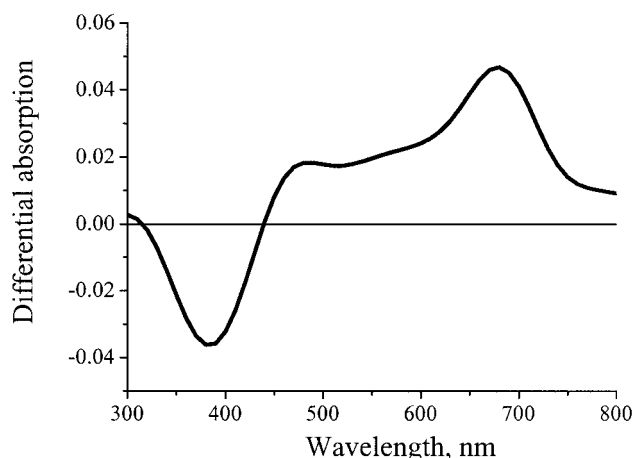


Figure 4. Transient differential absorption profile of **1** in acetonitrile, collected 100 ns after laser excitation with a 10-ns pulse

## Conclusion

The linking of two pyrene units via a butadiynylene bridge produces a highly fluorescent system which displays photophysical properties more akin to a single entity. The compound is robust and does not show any appreciable degradation under exposure to light in the presence of molecular oxygen. The attractive properties of the small array bodies well for its use in more complex assemblies as, for example, a fluorescent reporter in a chemical sensor. It is important to note that the fluorescence yield and lifetime remain insensitive to changes in solvent polarity and oxygen pressure. The red-shifted UV/visible absorption spectrum is more amenable to excitation with a dye laser and the compound is photostable. The most interesting features of **1** are the absence of excimer formation and the high fluorescence yield. Compound **1** can also behave in the singlet state as both a photooxidant ( $E_{ox}$  approximately equal to +1.4 eV) and photoreductant ( $E_{red}$  approximately equal to -1.1 eV), which is in complete contrast to pyrene which can only undergo a reductive electron transfer process. This compound can be functionalized; for example, sulfonation under mild conditions gives a water-soluble derivative, and is currently under investigation. The same strategy can be used with other aromatic polycycles, notably perylene, to produce a range of intensely fluorescent dyes that cover an unusually wide absorption and fluorescence spectral window.

## Experimental Section

**General Remarks:** High purity solvents for spectroscopic measurements were purchased from Aldrich Chemical Co. and, unless stated otherwise, were used as received. Butyronitrile was dried over CaH<sub>2</sub> and distilled under N<sub>2</sub> before use. The title compound **1** was prepared by modification of the literature procedure<sup>[16]</sup> as outlined below.

**1,4-Di(1-pyrenyl)butadiynylene (1):** Cupric acetate monohydrate (4.56 g, 2.07 mmol) was added to a stirred solution of 1-ethynylpyrene (460 mg, 23 mmol) in pyridine (20 mL). The mixture was stirred for 3 hours at 55 °C. The insoluble material which was deposited on cooling the reaction mixture was collected by filtration, and washed successively with methanol (100 mL) and water (100 mL) to give a deep yellow solid. The crude material was purified by at least two column chromatography separations (silica gel, petroleum ether {boiling range 40–60 °C} / ethyl acetate 19:1) to yield 325 mg (36%) of the desired product as a yellow solid. Samples for fluorescence measurements were purified by preparative TLC on silica using the same solvent mixture. M.p. > 250 °C. <sup>1</sup>H NMR (300 MHz, CDCl<sub>3</sub>): δ = 8.19 (m, 16 H), 8.73 (d, *J* = 9.1 Hz, 2 H). <sup>13</sup>C NMR (75.5 MHz, CDCl<sub>3</sub>): δ = 80.2 (2C), 83.1 (2C), 116.6 (2C), 124.4 (2C), 124.6 (2C), 124.8 (2C), 124.9 (2C), 125.8 (2C), 126.3 (2C), 126.3 (2C), 126.8 (2C), 127.6 (2C), 129.2 (2C), 129.3 (2C), 130.9 (2C), 131.4 (2C), 132.1 (2C), 133.7 (2C). HR-MS calculated for C<sub>36</sub>H<sub>18</sub>: 450.1409. Found: 450.1423. Elemental analysis calcd. (found) C, 95.97 (95.60), H 4.03 (4.43). Although the analysis for carbon and hydrogen is within 0.4%, the absolute purity of **1** was established by fluorescence spectroscopy which is significantly more sensitive to impurities (see text).

Cyclic voltammetric experiments were performed using a fully automated HCH Instruments Electrochemical Analyzer, and a three electrode set-up consisting of a glassy carbon working electrode, a platinum wire counter electrode and an Ag/AgCl reference electrode. All studies were performed in either deoxygenated acetonitrile or DMF containing tetra-*N*-butylammonium tetrafluoroborate (0.2 mol dm<sup>-3</sup>) as the background electrolyte. The concentration of **1** was typically 0.5 mM. Reduction potentials were reproducible to within ±15 mV.

Absorption spectra were recorded with a Hitachi U3310 spectrophotometer and emission spectra were recorded with a Hitachi F-4500 spectrofluorimeter. The molar absorption coefficient was measured by weighing small amounts of the target compound on a microbalance and diluting to the preset volume. Fluorescence spectra were fully corrected for imperfections of the instrument by reference to a standard lamp. All emission spectra were recorded for optically dilute solutions. Fluorescence quantum yields were determined relative to 9,10-diphenylanthracene (Φ<sub>F</sub> = 0.83)<sup>[23]</sup> in deoxygenated cyclohexane. Where necessary, changes in the refractive index were taken into consideration.<sup>[24]</sup> Concentration dependence studies were made with quartz cuvettes of differing pathlength. Phosphorescence spectra were recorded in the presence of 20% (v/v) iodoethane as the heavy-atom perturber. The solution was cooled to 77 K and examined with a gated flash lamp in order to exclude residual fluorescence. Fluorescence lifetimes were measured with a Yvon–Jobin tau-3 fluorolog spectrometer.

Laser flash photolysis studies were made with a Q-switched, frequency-tripled Nd-YAG laser (λ = 355 nm; FWHM = 10 ns). The solution was adjusted to possess an absorbance of 0.18 at 355 nm and was deoxygenated by bubbling with argon. The monitoring beam was provided by a pulsed Xe arc lamp and, after passage

through the sample, was directed to a high-radiance monochromator and then to a fast-response PMT. Transient differential absorption spectra were recorded point-by-point and were corrected for small changes in laser intensity. Kinetic measurements were recorded at a fixed wavelength, using signal averaging techniques. A fresh aliquot of solution was used for each laser shot.

Semi-empirical calculations were made at the PM3 level using the Gaussian-03 package. The ground-state structure was optimized both in vacuo and in a bath of acetonitrile as an inert solvent. The energy was minimized and single-point calculations performed for this geometry using the PM3 model Hamiltonians. The LUMO and HOMO were visualized for the fully optimized structure. The dihedral angle was varied manually, with the structure for the rest of the molecule being optimized. The energy was computed at the PM3 level for each angle.

## Acknowledgments

We thank the EPSRC (GR/S00088) and the University of Newcastle for their financial support of this work.

- [1] [1a] A. S. M. Dyck, U. Kisiel, C. Bohne, *J. Phys. Chem. B* **2003**, *107*, 11652. [1b] H. Wang, Y. Fang, L. Ding, L. Gao, D. Hu, *Thin Solid Films* **2003**, *440*, 255. [1c] Y. Mori, H. Shinoda, T. Nakano, K. Kitagawa, *J. Photochem. Photobiol. A-Chem.* **2003**, *157*, 33.
- [2] A.-J. Tong, A. Yamauchi, T. Hayashita, Z.-Y. Zhang, R. D. Smith, N. Termae, *Anal. Chem.* **2001**, *73*, 1530.
- [3] J. S. Kim, O. J. Shon, J. A. Rim, S. K. Kim, J. Yoon, *J. Org. Chem.* **2002**, *67*, 2348.
- [4] A. Corma, M. S. Galletero, H. García, E. Palomares, F. Rey, *Chem. Commun.* **2002**, 1100.
- [5] Y. Fujiwara, I. Okura, T. Miyashita, Y. Amao, *Anal. Chim. Acta* **2002**, *471*, 25.
- [6] L. J. D'Souza, U. Maitra, *J. Org. Chem.* **1996**, *61*, 9494.
- [7] D. Y. Sakaki, B. E. Padilla, *Chem. Commun.* **1998**, 1581.
- [8] J. L. Sessler, Y. Kubo, A. Harriman, *J. Phys. Org. Chem.* **1992**, *5*, 644.
- [9] [9a] G. Jones II, V. I. Vullev, *J. Phys. Chem. A* **2001**, *105*, 6402. [9b] J. M. G. Martinho, J. C. Conte, *J. Chem. Soc., Faraday Trans. II* **1982**, 975.
- [10] [10a] M. Okamoto, F. Tanaka, *J. Phys. Chem. A* **2002**, *106*, 3982. [10b] W. Xu, R. Schmidt, M. Whaley, J. N. Demas, B. A. DeGraff, E. K. Karikari, B. L. Farmer, *Anal. Chem.* **1995**, *67*, 3172.
- [11] K. Kalyanasundaram, J. K. Thomas, *J. Am. Chem. Soc.* **1977**, *99*, 2039.
- [12] S. Nishizawa, Y. Kato, N. Teramae, *J. Am. Chem. Soc.* **1999**, *121*, 9463.
- [13] [13a] L. Li, Z. Zhang, W. Long, A. Tong, *Spectrochim. Acta Part A* **2001**, *56*, 385. [13b] C. A. Parker, L. G. Hatchard, *Trans. Faraday Soc.* **1963**, *59*, 284.
- [14] [14a] L. Yao, L. Yiting, K. S. Schanze, *J. Photochem. Photobiol. C-Photochem. Rev.* **2000**, *3*, 1. [14b] K. D. Ley, C. Whittle, M. D. Bartberger, K. S. Schanze, *J. Am. Chem. Soc.* **1997**, *119*, 3423.
- [15] D. L. Pearson, J. M. Tour, *J. Org. Chem.* **1997**, *62*, 1376.
- [16] K. Nakasuji, S. Akiyama, M. Nakagawa, *Bull. Chem. Soc. Jpn.* **1972**, *45*, 875.
- [17] M. Hissler, A. Harriman, A. Khatyar, R. Ziessel, *Chemistry: Eur. J.* **1999**, *5*, 3366.
- [18] A. Harriman, M. Hissler, R. Ziessel, *Phys. Chem. Chem. Phys.* **1999**, *1*, 4203.
- [19] A. C. Benniston, A. Harriman, D. J. Lawrie, A. Mayeux, *Phys. Chem. Chem. Phys.* **2004**, *6*, 51.

- <sup>[20]</sup> P. Reynders, W. Kühnle, K. A. Zachariasse, *J. Phys. Chem.* **1990**, *94*, 4073.
- <sup>[21]</sup> <sup>[21a]</sup> T. Asahi, N. Mataga, *J. Phys. Chem.* **1989**, *93*, 6575. <sup>[21b]</sup> H. Segwa, C. Takehara, K. Honda, T. Shimidzu, T. Asahi, N. Mataga, *J. Phys. Chem.* **1992**, *96*, 503. <sup>[21c]</sup> R. Englman, J. Jortner, *J. Mol. Phys.* **1970**, *18*, 145.
- <sup>[22]</sup> G. W. Byers, S. Gross, P. M. Henrichs, *Photochem. Photobiol.* **1976**, *23*, 37.
- <sup>[23]</sup> S.L. Murov, *Handbook of Photochemistry*, Dekker, New York, **1973**.
- <sup>[24]</sup> J. B. Birks, *Photophysics of Aromatic Molecules*, Wiley Interscience, London, **1970**.

Received January 15, 2004